Available online at www.sciencedirect.com
SCIENCE DIRECT®
Journal of Photochemistry and Photobiology A: Chemistry 162 (2004) 273–281
Journal of Photochemistry and Photobiology A:Chemistry
www.elsevier.com/locate/jphotochem

UV-absorption cross sections of benzaldehyde, ortho-, meta-, and para-tolualdehyde

G. Thiault [a], A. Mellouki [a,*], G. Le Bras [a], A. Chakir [b], N. Sokolowski-Gomez [b], D. Daumont [b]

[a] *LCSR/CNRS, 1C Avenue de la recherche scientifique, 45071, Orléans Cedex 02, France*
[b] *GSMA/CNRS UMR 6089, UFR Sciences, BP 1039, 51687, Reims Cedex 02, France*

Received 7 May 2003; received in revised form 27 August 2003; accepted 27 August 2003

Abstract

Absorption cross-sections for benzaldehyde, *o*-tolualdehyde, *m*-tolualdehyde and *p*-tolualdehyde have been measured in the wavelength region 252–368 nm using two different systems (D_2 lamp-diode array and D_2 lamp-monochromator). In addition, cross sections at 253.7, 312.2 and 365 nm have been measured using a Hg pen ray lamp and were found in good agreement with those obtained using the D_2 lamp-diode array system. The absorption spectra of the four aromatic aldehydes have been found to exhibit fine structures similarly to aromatic hydrocarbons. The calculated atmospheric photolysis lifetimes suggest that photolysis is a potentially important removal process for these aromatic aldehydes in the troposphere.

Keywords: UV spectra; benzaldehyde; *o*-Tolualdehyde; *m*-Tolualdehyde; *p*-Tolualdehyde

1. Introduction

Aromatic aldehydes are emitted into the atmosphere as primary pollutants from motor vehicles exhaust and through their different uses (e.g. soil fumigant) [1]. They are also produced in situ in the atmosphere as intermediates in the photooxidation of alkyl aromatic compounds such as toluene, xylenes and styrenes [2–6]. Similarly to other aromatics, these compounds play an important role in urban air pollution [7]. The available literature data indicate that in the atmosphere, the main oxidation processes of aromatic aldehydes in the gas phase are reaction with OH radicals and photolysis [3,6].

The UV absorption cross sections of aromatic aldehydes combined with photolysis quantum yields are necessary to calculate the photolysis rates of these compounds in the laboratory and in the atmosphere. They are also required for in situ detection of these species in the atmosphere for example, by using the differential optical absorption spectroscopy (DOAS) technique [8,9]. The UV absorption spectra of benzaldehyde have been determined previously by different groups but a large discrepancy exists between some of these measurements [8–11].

In the present study, the absorption cross sections for benzaldehyde (C_6H_5CHO), ortho-tolualdehyde (*o*-$CH_3C_6H_4CHO$), meta-tolualdehyde (*m*-$CH_3C_6H_4CHO$) and para-tolualdehyde (*p*-$CH_3C_6H_4CHO$) have been determined in the wavelength range 252–368 nm and temperatures between 303 and 363 K, by using two different experimental systems.

2. Experimental

Absorption cross sections measurements were made in two different tubular cells using D_2 lamp as the light source and a diode-array spectrometer at LCSR-Orléans and a monochromator at GSMA-Reims for light detection. A brief description of both systems is given here, however, complete details can be found elsewhere [12,13].

2.1. D_2 lamp-diode array system at LCSR-Orléans

The used UV-Vis spectrophotometer is equipped with a 1800 grooves/mm grating and a 1024 element diode array detector. The collimated output of D_2 lamp (30 W) passed through the absorption cell and focused onto the entrance slit of the spectrometer. The absorption cell (100 cm long

* Corresponding author. Tel.: +33-238-25-7612; fax: +33-238-69-6004.
E-mail address: mellouki@cnrs-orleans.fr (A. Mellouki).

1010-6030/$ – see front matter © 2004 Elsevier B.V. All rights reserved.
doi:10.1016/j.nainr.2003.08.012

and 2.5 cm i.d.) made of Pyrex is equipped with quartz windows, the temperature is regulated by circulating heated water through the cell jacket. Experiments were conducted with a 40 μm entrance slit, providing a spectral resolution of 0.2 nm. Measurements were made over the wavelength range 252–368 nm by recording typically four overlapping regions of about 40 nm. Each measurement consisted of 10–20 scans of diode array and required at maximum 1 s to complete. The wavelength scale of the spectrometer was calibrated using the emission lines from low-pressure Zn (213.8 nm) and Hg (253.7, 313.3, and 365 nm) pen-ray lamps and it was found to be accurate to 0.1 nm.

2.2. D_2 lamp-monochromator system at GSMA-Reims

The difference between this experimental set-up and that described above are the length of the cell (here 49.6 cm) and the light detection (here a monochromator was used instead of a diode-array). The monochromator used is a 1.5 m Jobin Yvon THR equipped with a 2400 line mm^{-1} grating (dispersion 0.26 nm mm^{-1}). The signal was collected by a photomultiplier tube (Hamamatsu R955) connected to a microcomputer for the data acquisition. The width of the entrance light beam was varied between 80 and 180 μm yielding a spectral resolution between 0.02 and 0.05 nm. For each scan, the integration time at each wavelength was 0.5 s and the experimental sampling was varied between 0.05 and 0.2 nm. The wavelength calibration was made using a low pressure mercury lamp and the precision was estimated to be better than ±0.02 nm. The absorption cross sections were measured between 252 and 295 nm under static conditions in the temperature range 353–363 K using a resistor to heat the cell.

Absorption cross sections were calculated using the Beer–Lambert's law:

$$\sigma(\lambda) = -\ln[I(\lambda)/I_0(\lambda)]/LC,$$

where $\sigma(\lambda)$ is the absorption cross section (cm^2 per molecule) at wavelength λ, L the optical path length in cm and C the concentration in molecule cm^{-3}. $I(\lambda)$ and $I_0(\lambda)$ are respectively the light intensities with and without aromatic aldehydes in the absorption cell.

A reference spectrum, $I_0(\lambda)$ was recorded when the cell was empty after being purged with He. The spectrum $I(\lambda)$ was measured by two methods. In the so-called static method, $I(\lambda)$ was measured when the absorption cell was filled with a fixed concentration of aromatic aldehyde, while in the second method, called dynamic, $I(\lambda)$ was measured when a fixed concentration of compound was flowed through the absorption cell. This procedure was repeated until sufficient spectra were recorded to accurately determine the absorption cross section at all wavelengths. Following each measurement, the cell was evacuated and purged with He and another $I_0(\lambda)$ spectrum was recorded to check the stability of the apparatus over the duration of the experiments.

Pressure was measured in both systems using capacitance manometers operating in the range 0–10 Torr. The chemicals were from Fluka and their purities were as follows: benzaldehyde (≥99%), *o*-tolualdehyde (≥98%), *m*-tolualdehyde (99%) and *p*-tolualdehyde (98%). They were purified by repeat freeze, pump, and thaw cycles. In addition, the compounds were further purified by distillation in the experiments conducted at GSMA.

3. Results and discussion

3.1. Results

Preliminary checks showed that in our experimental conditions, a slight photolysis of the studied compounds occurred when they were irradiated at wavelengths below 240 nm. Therefore, all measurements were conducted in the presence of a band-pass filter between the D_2 lamp and the absorption cell, hence allowing only radiation at $\lambda > 245$ nm to pass through. At LCSR, absorption spectra of benzaldehyde, *o*-tolualdehyde, *m*-tolualdehyde and *p*-tolualdehyde were measured between 252 and 368 nm in the temperature range 303–333 K while at GSMA experiments were performed in the wavelength and temperature ranges 252–295 nm and 353–363 K, respectively. The experiments were conducted at temperatures above 303 K, in order to minimize the loss of the studied compounds on the wall of the cell. The experiments conducted at around 295 K showed that the compounds had a tendency to be lost on the wall of the absorption cell and the data obtained were not reproducible. Hence, the results obtained at 295 K could not be used.

Measurements of the absorption spectra were conducted at different pressures as follows: at LCSR, at least four independent measurements in static and two in dynamic conditions in the pressure range 0.2–0.8 Torr; at GSMA five to seven measurements in static conditions in the pressure range 0.1–2.2 Torr in static conditions. Uncertainties in the aromatic aldehydes cross section data arise from errors mainly in pressure measurements and to a lesser extent in absorbance, path length and temperature measurements. Estimated uncertainties for the cross sections are ±15% below 340 nm, and ±20% above. The spectra obtained at LCSR and GSMA are plotted in Fig. 1 and the cross sections values are listed in Table 1 in 1 nm intervals.

Independent experiments were conducted at LCSR to measure the absorption cross sections of the studied aromatic aldehydes at 253.7, 313.2 and 365 nm using a Hg pen ray lamp as the light source and a photodiode fitted with appropriate band-pass filters for detection. These experiments were carried out at 323 K and pressure range of 0.1–0.8 Torr. The absorption cross sections obtained in this way shown in Fig. 2 and those obtained using the D_2 lamp-diode array system are in good agreement as presented in Table 2.

Table 1
Absorption cross sections of benzaldehyde, *o*-tolualdehyde, *m*-tolualdehyde and *p*-tolualdehyde obtained using D_2 lamp-diode array (LCSR) and D_2 lamp-monochromator (GSMA) systems

λ	Benzaldehyde		*o*-Tolualdehyde		*m*-Tolualdehyde		*p*-Tolualdehyde	
	LCSR	GSMA	LCSR	GSMA	LCSR	GSMA	LCSR	GSMA
σ (10^{-18} cm^2 per molecule)								
252	0.80	0.80	2.04	2.96	0.97	1.09	9.98	10.1
253	0.81	0.81	1.40	2.19	0.74	0.94	7.93	8.10
254	0.84	0.82	0.97	1.58	0.61	0.83	5.41	5.50
255	0.92	0.88	0.74	1.22	0.55	0.80	3.78	3.93
256	1.00	0.93	0.62	1.0	0.52	0.80	2.68	2.87
257	1.06	0.95	0.57	0.89	0.53	0.79	2.16	2.31
258	1.14	1.05	0.57	0.84	0.55	0.83	1.74	1.92
259	1.22	1.11	0.58	0.84	0.58	0.85	1.57	1.69
260	1.30	1.25	0.62	0.83	0.62	0.88	1.46	1.60
261	1.34	1.35	0.66	0.86	0.67	0.91	1.38	1.51
262	1.42	1.42	0.71	0.90	0.72	0.96	1.32	1.55
263	1.49	1.53	0.77	0.95	0.78	1.0	1.38	1.53
264	1.54	1.65	0.83	1.0	0.85	1.04	1.35	1.52
265	1.64	1.75	0.91	1.06	0.91	1.09	1.42	1.65
266	1.75	1.85	0.99	1.13	0.98	1.15	1.44	1.51
267	1.88	1.84	1.07	1.20	1.06	1.20	1.38	1.57
268	1.85	2.0	1.17	1.29	1.14	1.27	1.46	1.54
269	1.87	2.04	1.26	1.37	1.22	1.34	1.38	1.48
270	1.99	2.11	1.36	1.47	1.34	1.41	1.43	1.56
271	2.11	2.17	1.47	1.57	1.44	1.45	1.48	1.55
272	2.12	2.38	1.57	1.67	1.53	1.55	1.44	1.54
273	2.10	2.35	1.68	1.77	1.60	1.61	1.66	1.74
274	2.19	2.43	1.79	1.89	1.69	1.67	1.60	1.64
275	2.27	3.80	1.88	1.98	1.75	1.74	1.51	1.53
276	2.06	2.52	1.96	2.04	1.79	1.77	1.58	1.63
277	2.28	2.56	2.09	2.19	1.85	1.84	1.33	1.37
278	2.20	2.63	2.14	2.26	1.95	1.88	1.27	1.27
279	1.70	1.83	2.29	2.37	2.05	1.99	1.34	1.42
280	1.72	1.79	2.39	2.51	2.11	2.06	1.15	1.19
281	2.10	1.38	2.46	2.51	2.22	2.15	1.06	1.13
282	1.64	1.72	2.56	2.55	2.30	2.22	1.10	1.27
283	1.74	1.73	2.61	2.71	2.22	2.13	1.06	1.03
284	2.40	2.02	2.53	2.67	2.15	2.15	1.17	1.04
285	1.54	2.10	2.37	2.50	2.08	2.10	1.16	1.56
286	0.84	1.21	2.45	2.52	1.91	1.92	0.69	1.05
287	0.56	0.70	2.34	2.62	1.78	1.81	0.42	0.66
288	0.37	0.48	2.26	2.39	1.81	1.72	0.28	0.41
289	0.24	0.30	2.42	2.48	1.89	1.83	0.21	0.33
290	0.15	0.16	2.19	2.43	1.85	1.78	0.15	0.26
291	0.12	0.11	2.09	2.18	1.80	1.78	0.10	0.22
292	0.10	0.08	2.55	2.32	1.91	2.19	0.08	0.19
293	0.087	0.072	2.11	2.56	1.82	2.08	0.067	0.14
294	0.065	0.058	1.46	1.97	1.31	1.44	0.058	0.15
295	0.059	0.050	1.12	1.42	0.82	0.95	0.054	0.14
296	0.053	–	1.04	–	0.54	–	0.048	–
297	0.049	–	0.88	–	0.37	–	0.043	–
298	0.047	–	0.56	–	0.25	–	0.040	–
299	0.047	–	0.36	–	0.17	–	0.039	–
300	0.047	–	0.22	–	0.11	–	0.039	–
301	0.049	–	0.14	–	0.082	–	0.039	–
302	0.051	–	0.10	–	0.063	–	0.041	–
303	0.055	–	0.076	–	0.051	–	0.043	–
304	0.058	–	0.059	–	0.044	–	0.045	–
305	0.060	–	0.049	–	0.039	–	0.046	–
306	0.058	–	0.042	–	0.036	–	0.045	–
307	0.053	–	0.039	–	0.034	–	0.044	–
308	0.051	–	0.036	–	0.032	–	0.042	–
309	0.049	–	0.034	–	0.031	–	0.040	–
310	0.051	–	0.031	–	0.029	–	0.040	–

Table 1 (*Continued*)

λ	Benzaldehyde		*o*-Tolualdehyde		*m*-Tolualdehyde		*p*-Tolualdehyde	
	LCSR	GSMA	LCSR	GSMA	LCSR	GSMA	LCSR	GSMA
311	0.056	–	0.030	–	0.027	–	0.042	–
312	0.060	–	0.030	–	0.026	–	0.043	–
313	0.066	–	0.030	–	0.025	–	0.046	–
314	0.069	–	0.030	–	0.026	–	0.049	–
315	0.071	–	0.031	–	0.027	–	0.051	–
316	0.068	–	0.031	–	0.029	–	0.053	–
317	0.063	–	0.031	–	0.030	–	0.052	–
318	0.062	–	0.031	–	0.031	–	0.050	–
319	0.058	–	0.030	–	0.031	–	0.048	–
320	0.058	–	0.029	–	0.030	–	0.055	–
321	0.063	–	0.029	–	0.029	–	0.044	–
322	0.067	–	0.029	–	0.028	–	0.045	–
323	0.072	–	0.030	–	0.027	–	0.046	–
324	0.069	–	0.031	–	0.026	–	0.048	–
325	0.070	–	0.031	–	0.027	–	0.049	–
326	0.072	–	0.032	–	0.028	–	0.048	–
327	0.082	–	0.032	–	0.029	–	0.048	–
328	0.074	–	0.031	–	0.029	–	0.052	–
329	0.067	–	0.031	–	0.029	–	0.053	–
330	0.061	–	0.030	–	0.030	–	0.048	–
331	0.058	–	0.030	–	0.030	–	0.046	–
332	0.062	–	0.029	–	0.029	–	0.043	–
333	0.062	–	0.029	–	0.026	–	0.043	–
334	0.075	–	0.028	–	0.025	–	0.043	–
335	0.075	–	0.028	–	0.025	–	0.048	–
336	0.078	–	0.028	–	0.026	–	0.048	–
337	0.072	–	0.028	–	0.026	–	0.049	–
338	0.058	–	0.029	–	0.030	–	0.045	–
339	0.058	–	0.029	–	0.030	–	0.042	–
340	0.056	–	0.029	–	0.027	–	0.040	–
341	0.056	–	0.029	–	0.026	–	0.039	–
342	0.046	–	0.028	–	0.023	–	0.043	–
343	0.041	–	0.026	–	0.022	–	0.041	–
344	0.041	–	0.025	–	0.022	–	0.039	–
345	0.037	–	0.024	–	0.021	–	0.034	–
346	0.045	–	0.023	–	0.019	–	0.031	–
347	0.052	–	0.023	–	0.017	–	0.030	–
348	0.054	–	0.022	–	0.015	–	0.030	–
349	0.071	–	0.020	–	0.014	–	0.031	–
350	0.065	–	0.020	–	0.015	–	0.034	–
351	0.052	–	0.019	–	0.016	–	0.033	–
352	0.046	–	0.019	–	0.019	–	0.046	–
353	0.034	–	0.019	–	0.020	–	0.031	–
354	0.029	–	0.020	–	0.024	–	0.028	–
355	0.031	–	0.020	–	0.017	–	0.025	–
356	0.030	–	0.018	–	0.013	–	0.019	–
357	0.030	–	0.019	–	0.010	–	0.017	–
358	0.022	–	0.016	–	0.007	–	0.017	–
359	0.019	–	0.014	–	0.007	–	0.019	–
360	0.024	–	0.014	–	0.006	–	0.017	–
361	0.023	–	0.012	–	0.005	–	0.013	–
362	0.023	–	0.011	–	0.005	–	0.011	–
363	0.026	–	0.010	–	0.006	–	0.010	–
364	0.023	–	0.009	–	0.005	–	–	–
365	0.024	–	0.008	–	0.005	–	–	–
366	0.031	–	0.007	–	0.005	–	–	–
367	0.016	–	0.007	–	0.006	–	–	–
368	0.016	–	0.007	–	0.005	–	–	–

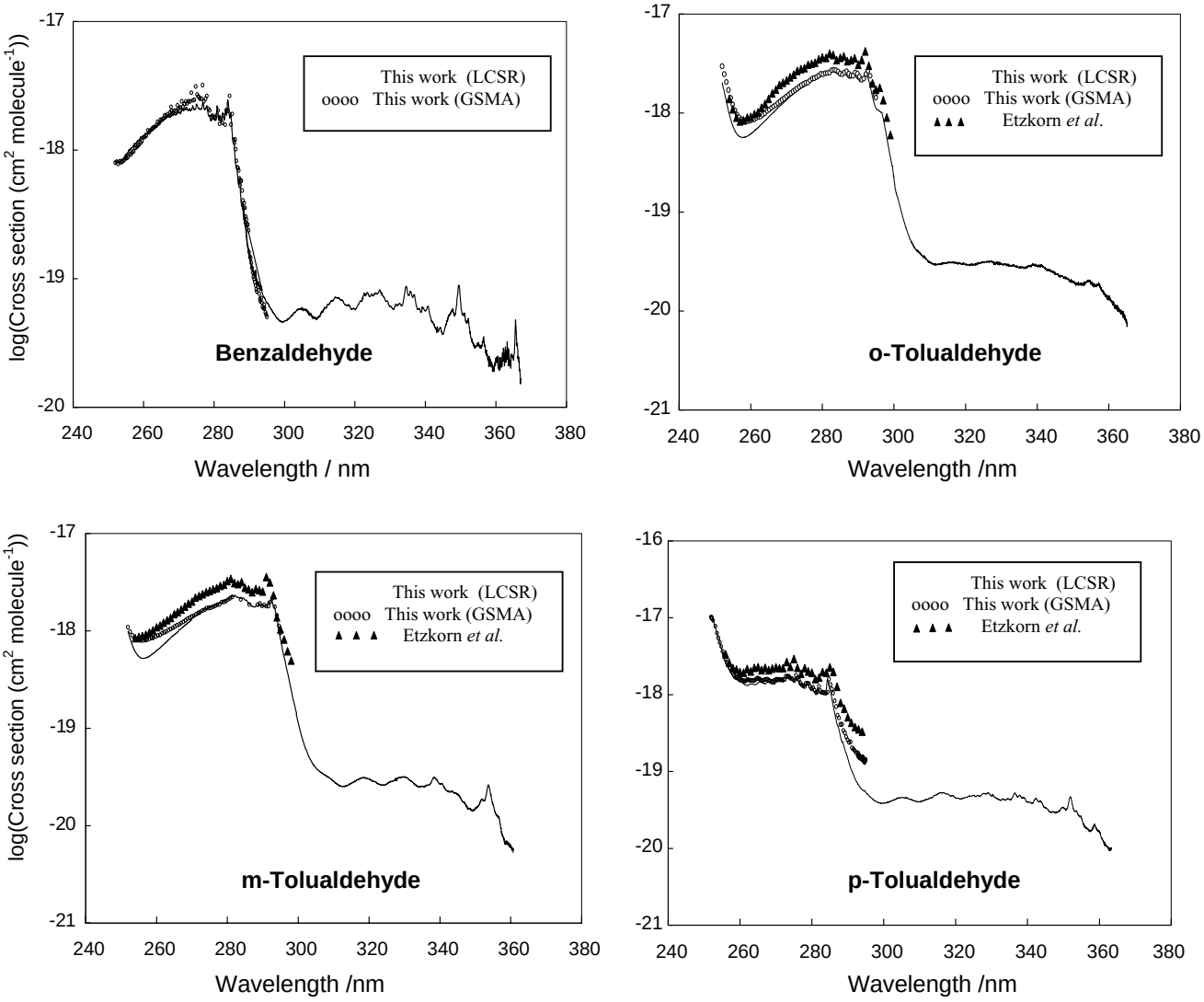

Fig. 1. UV-Vis spectra of benzaldehyde, *o*-tolualdehyde, *m*-tolualdehyde and *p*-tolualdehyde obtained in this work (GSMA and LCSR) and those from Etzkorn et al. [9].

3.2. Intercomparison of the LCSR and GSMA data

As shown in Fig. 1, the spectra of *o*- and *m*-tolualdehyde are similar in terms of cross sections values, peaks position and band widths while that of *p*-tolualdehyde is shifted to shorter wavelengths similarly to that of benzaldehyde. This shift has also been observed for benzene compared to toluene [9]. The four absorption spectra exhibit fine structures similarly to other aromatics [9]. As expected for carbonyls, the absorption bands between 320 and 360 nm result from a dipole forbidden n–π* electronic transition of the C=O group.

The cross section values for benzaldehyde and *p*-tolualdehyde obtained at LCSR and GSMA are within the reported uncertainties except for *p*-tolualdehyde at wavelength higher than 290 nm where the disagreement exceeds 40%. Additionally, the fine structures are more defined in the spectra obtained at GSMA because of the better resolution of the system used in this laboratory. It has to be noticed that a slight shift (0.2–0.4 nm) is observed between the spectra obtained in the two laboratories.

For *o*-tolualdehyde and *m*-tolualdehyde, the results from the two laboratories are in reasonable agreement except for the wavelength region 254–262 nm where the absorption cross section values from LCSR are up to 40% lower than those from GSMA. We have no evident explanation for this disagreement, which might be due to light scattering in the monochromator and the cells or to the presence of impurities that would absorb in that wavelength region.

Additionally, the measured absorption cross sections did not show any distinct temperature dependence in the temperature range (303–363 K) of this study.

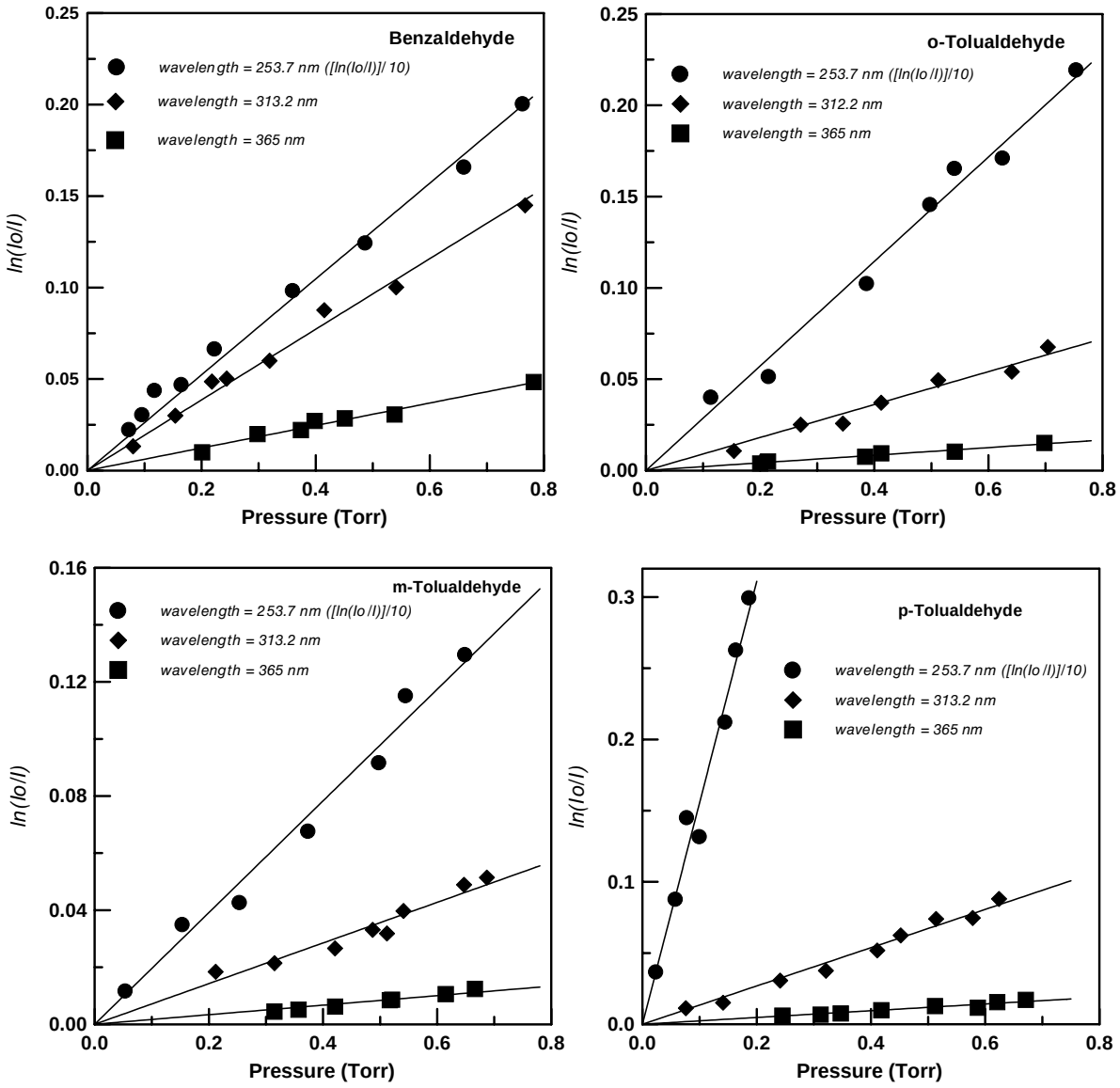

Fig. 2. Optical density vs. pressure plots for benzaldehyde, *o*-tolualdehyde, *m*-tolualdehyde and *p*-tolualdehyde at $\lambda = 253.7$, 313.2 and 365 nm (the derived absorption cross sections are given in Table 2).

3.3. Comparison with the literature data

The data obtained in this work can also be compared with those of the literature. For benzaldehyde, Nozière et al. [10] have determined its spectrum between 220 and 300 nm in 5 nm or 10 nm intervals using a D_2 lamp coupled to a monochromator. As shown in Fig. 3, the data obtained in this work disagree with those reported by these authors. Our cross section values are three times lower in the region 255–280 nm and 14-35 times lower between 290 and 300 nm. Because of a lack of experimental details in the paper of Nozière et al. [10], it is difficult to discuss this discrepancy. However, it is not excluded that their data were affected by absorbing products formed in the possible photolysis of aromatic aldehydes at wavelengths shorter than 240 nm as observed in this work. The UV absorption spectra of benzaldehyde has also been reported by Etzkorn et al. in the wavelength range 250–300 nm using a diode array with a spectral resolution of 0.146 nm [9]. Our cross section values can be considered in agreement with those from Etzkorn et al., within 5–25% in the wavelength range 255–292 nm [9]. More recently, Zhu and Cronin [11] have measured the absorption cross sections of benzaldehyde at three wavelengths (280, 285 and 308 nm). Our value at 308 nm ($\sigma_{308} = (5.1 \pm 0.8) \times 10^{-20}$ cm^2 per molecule) is close (30% higher) to their determination $(3.8 \pm 0.9) \times 10^{-20}$, but our values at 280 and 285 nm ($\sigma_{280} = (1.76 \pm 0.26) \times 10^{-18}$ and $\sigma_{285} = (1.82 \pm 0.27) \times 10^{-18}$) are, respectively, 10 and 5 times higher than theirs ($(1.8 \pm 0.4) \times 10^{-19}$ and $(3.2 \pm 0.9) \times 10^{-19}$ cm^2 per molecule).

Table 2
Comparison of the absorption cross section for the series of aromatic aldehydes at 253.7, 313.2 and 365 nm obtained by using Hg lamp-photodiode or D_2 lamp-diode array

Aromatic aldehydes	σ (253.7 nm)		σ (313.2 nm)		σ (365 nm)	
	Photodiode	Diode array	Photodiode	Diode array	Photodiode	Diode array
Benzaldehyde	$(8.5 \pm 1.3) \times 10^{-19}$	$(8.4 \pm 1.3) \times 10^{-19}$	$(6.6 \pm 0.1) \times 10^{-20}$	$(6.7 \pm 1.0) \times 10^{-20}$	$(2.2 \pm 0.4) \times 10^{-20}$	$(2.4 \pm 0.4) \times 10^{-20}$
o-Tolualdehyde	$(1.0 \pm 0.15) \times 10^{-18}$	$(1.1 \pm 0.2) \times 10^{-18}$	$(3.1 \pm 0.5) \times 10^{-20}$	$(3.0 \pm 0.5) \times 10^{-20}$	$(7.2 \pm 1.4) \times 10^{-21}$	$(7.7 \pm 1.2) \times 10^{-21}$
m-Tolualdehyde	$(6.6 \pm 0.1) \times 10^{-19}$	$(6.4 \pm 0.9) \times 10^{-19}$	$(2.4 \pm 0.4) \times 10^{-20}$	$(2.5 \pm 0.4) \times 10^{-20}$	$(5.4 \pm 1.0) \times 10^{-21}$	$(5.2 \pm 0.8) \times 10^{-21}$
p-Tolualdehyde	$(5.7 \pm 0.9) \times 10^{-18}$	$(6.0 \pm 0.9) \times 10^{-18}$	$(4.7 \pm 0.7) \times 10^{-20}$	$(4.6 \pm 0.7) \times 10^{-20}$	$(8.4 \pm 1.7) \times 10^{-21}$	–

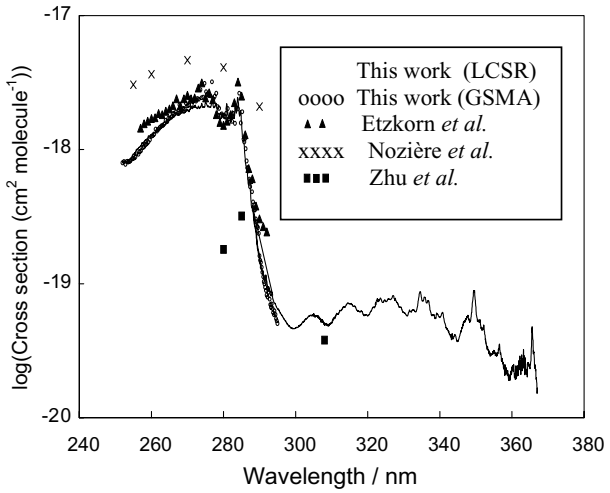

Fig. 3. UV-Vis spectra of benzaldehyde obtained in this work (GSMA and LCSR) and those from the literature.

Concerning the three tolualdehyde isomers, their UV absorption spectra have been reported earlier by Etzkorn et al. in the wavelength range 250–300 nm [9]. As shown in Fig. 1, while the shapes of the spectra from this work and from Etzkorn et al. are similar, our cross section values are systematically lower than those of Etzkorn et al. The reason for this systematic difference is not clear. However, it seems to indicate a possible problem with the concentration measurements of the tolualdehydes due to difficulties of handling the samples. The very recent data obtained by Volkamer et al. using a DOAS (resolution of 0.84 nm) are in agreement with those from this work for benzaldehyde but systematically higher for the tolualdehydes (Euphore Report, 2002).

4. Tropospheric lifetimes

The four aromatic aldehydes studied in this work show relatively high absorption cross sections for the wavelength around 300 nm which indicates that photolysis could be a significant loss process of these compounds in the troposphere.

The absorption cross-sections shown in Table 1 were used to calculate averaged tropospheric photolysis rate (J_p) for benzaldehyde, *o*-tolualdehyde, *m*-tolualdehyde and *p*-tolualdehyde by using the following relationship:

$$J_p = \int \sigma(\lambda)\phi(\lambda)I(\lambda)\,d\lambda$$

where $\sigma(\lambda)$ is the absorption cross section, $\phi(\lambda)$ the primary quantum yield for photolysis and $I(\lambda)$ the actinic flux of solar radiation. The calculations were made for noontime on 1 January and 1 July conditions, cloudless at sea level and at latitude of 40° N. The data for the actinic flux at the earth's surface and zenith angle ($\theta = 63°$ for 1 January and $\theta = 16.9°$ for 1 July) were taken from Demerjian et al. [14]. Calculations were made assuming $\phi(\lambda) = 1$ at all wavelengths since no data on the primary photolysis quantum yields are available which will lead to an upper limit of the calculated photodissociation rate. The calculated values of J_p (in s^{-1}) for 1 January and 1 July are, respectively, for benzaldehyde: 2.3×10^{-4} and 3.9×10^{-4}, for *o*-tolualdehyde: 1×10^{-4} and 2×10^{-4}, for *m*-tolualdehyde: 0.8×10^{-4} and 1.7×10^{-4} and for *p*-tolualdehyde: 1.5×10^{-4} and 2.8×10^{-4}.

Table 3
Estimated tropospheric lifetimes of the studied aromatic aldehydes in the gas phase with respect to photolysis, and reactions with OH and NO_3 radicals

	τ_J[a] (h)	τ_{OH} [17] (h)	τ_{NO_3} [3] (days)
Benzaldehyde	45 min[b]	11	2
o-Tolualdehyde	1.5	7	–
m-Tolualdehyde	2	8	–
p-Toluladehyde	1	10	–

[a] Lower limits (see text).
[b] Vaule for bezaldehyde is in minutes.

In the troposphere, aromatic aldehydes are expected to be removed in the gas phase by chemical reactions with OH, NO_3, and O_3 or by solar radiation photolysis. No data are available on the reactions of ozone with aromatic aldehydes but this process is expected to be negligible in the atmosphere [3,6]. The calculated lifetimes of the four aromatic aldehydes with respect to the different degradation pathways are listed in Table 3. The lifetimes with respect to the reaction with OH and NO_3 radicals have been calculated using rate constants of the literature and assuming $[OH] = 2 \times 10^6\ cm^{-3}$ and $[NO_3] = 2.5 \times 10^9\ cm^{-3}$ [15,16] which are typical for continental atmosphere where the studied aldehydes could be present. As mentioned above, the estimated lifetimes with respect to photolysis represent lower limits as they were calculated using the upper limits of J_p obtained assuming a photolysis quantum yield of unity (J_p are calculated for the 1 July). These calculations suggest that the photolysis is a potentially important loss process of the aromatic aldehydes in the troposphere compared to reactions with OH and NO_3 radicals. However, the photolysis rates of these aldehydes remain to be better defined to accurately assess their tropospheric lifetimes with respect to photolysis. In this respect, there is a need to determine the quantum yields for photolysis of these compounds and to measure their photolysis rates under simulated atmospheric conditions.

Acknowledgements

This work was supported by the Programme National de Chimie Atmosphérique (PNCA) of CNRS and the Environment Program of the European Union through the IALSI project (EVR1-CT-2001-40013). Thanks are due to Dr. R. Volkamer for providing us his data prior publication.

References

[1] C.L. Wilson, J.M. Solar, A. El Ghaouth, D.R. Fravel, Horthscience 34 (1999) 681–685.
[2] R. Atkinson, S.M. Aschmann, J. Arey, Int. J. Chem. Kinet. 23 (1991) 77.
[3] R. Atkinson, J. Phys. Chem. Ref. Data, Monograph No. 2, 1994.
[4] B. Klotz, S. Sorensen, I. Barnes, K.H. Becker, T. Etzkorn, R. Volkamer, U. Platt, K. Wirtz, M. Martin-Reviejo, J. Phys. Chem. A 102 (1998) 10289–10299.
[5] D.F. Smith, T.E. Kleindienst, C.D. McIver, J. Atmos. Chem. 34 (1999) 339–364.
[6] J.G. Calvert, R. Atkinson, K.H. Becker, R.M. Kamens, J.H. Seinfeld, T.J. Wallington, G. Yarwood, The Mechanisms of Atmospheric Oxidation of Aromatic Hydrocarbons, Oxford University Press, London, 2002.
[7] R. Derwent, M.E. Jenkin, S.M. Saunders, Atmos. Environ. 30 (1996) 191–199.
[8] J. Trost, J. Stutz, U. Platt, Atmos. Environ. 31 (1997) 3999–4008.
[9] T. Etzkorn, B. Klotz, S. Sorensen, I. Patroescu, I. Barnes, K.H. Becker, U. Platt, Atmos. Environ. 33 (1999) 525–540.
[10] B. Nozière, R. Lesclaux, M.D. Hurley, M.A. Dearth, T.J. Wallington, J. Phys. Chem. 98 (1994) 2864–2874.
[11] L. Zhu, T.J. Cronin, Chem. Phys. Lett. 317 (2000) 227–231.
[12] M. Yujing, A. Mellouki, J. Photochem. Photobiol. A: Chem. 134 (2000) 31–36.
[13] D. Daumont, J. Brion, J. Charbonnier, J. Malicet, J. Atmos. Chem. 15 (1992) 145–155.
[14] K.L. Demerjian, K.L. Schere, J.T. Peterson, Adv. Environ. Sci. Tech. 10 (1980) 369.
[15] R. Hein, P.J. Crutzen, M. Heinmann, Global Biogeochem. Cycles 11 (1997) 143.
[16] U. Platt, C. Janssen, Faraday Disc. 100 (1996) 175.
[17] G. Thiault, A. Mellouki, G. Le Bras, Phys. Chem. Chem. Phys. 4 (2002) 2194–2199.